

UNDRAINED RESPONSE OF LOOSE FIBER REINFORCED SAND

Devrim ERDOĞAN^{1*}, Selim ALTUN²

^{1,2} Ege Üniversitesi Mühendislik Fakültesi İnşaat Mühendisliği Bölümü, 35100, İzmir, TURKEY

Abstract: In the context of this paper, undrained response of fiber reinforced sands is investigated through consolidated undrained triaxial tests conducted under effective consolidation pressures of 50, 100 and 200 kPa. in loose state of the host sand ($D_r=25\%$) and at fiber concentrations of 0.5% and 1%. Results were challenging since addition of fiber reinforcement caused increased dilative tendency of the host sand giving way to considerable amount of decrease in excess pore water pressures which is advantageous for undrained loading conditions especially for earthquake loading conditions. This behaviour brought about the fact that both fiber phase and the sand matrix should be contributing to hydrostatic and deviatoric stress states of the fiber reinforced samples which was also proved very recently by a couple of researchers in the literature.

Keywords: fiber reinforced sand, drained and undrained triaxial testing

FİBER KATKILI KUMLARIN DRENAJSIZ KOŞULLARDAKİ KAYMA DAYANIMI DAVRANIŞI

Özet: Bu çalışma kapsamında fiber katkıli gevşek ($D_r=25\%$) suya doymun kumların drenajsız yükleme koşulları altındaki davranışları konsolidasyonlu drenajsız üç eksenli basınç deneyleri ile incelenmiştir. Deneyler 50, 100 ve 200 kPa efektif konsolidasyon basınçları altında ve %0.5 ile %1 fiber katkıli durumları için gerçekleştirilmiştir. Deney sonuçları fiber katkısının gevşek kumların drenajsız koşullardaki kayma dayanımı davranışında iyileşme sağlandığını göstermiştir. Deneylerde gözlemlenen ilginç bir sonuç, çoğu örnekte drenajsız kesme koşullarında elde edilen hacim değişimi eğilimlerinin genellikle hacim artışı ve dolayısı ile aşırı boşluk suyu basınçlarını azaltıcı yönde gerçekleşmiş olmasıdır. Aşırı boşluk suyu basınçlarındaki azalma efektif gerilmelerin ve dolayısı ile kayma dayanımının artışına olanak sağlamaktadır ki deprem durumundaki yükleme koşulları için elverişli bir durumdur. Ancak fiber katkıli kumların hacim değişimi eğilimleri ile ilgili olarak literatürde çok az çalışma bulunmaktadır. Bu deneysel çalışmada elde edilen sonuçlar, kum matrisi ve fiber fazının, deviatorik ve hacimsel davranışa ayrı ayrı katkı yaptıklarını göstermiştir.

Anahtar kelimeler: fiber katkıli kum, drenajlı ve drenajsız üç eksenli basınç deneyleri

1. INTRODUCTION

Fiber reinforced soil which is a mechanical means of soil reinforcement may be one of the most practical reinforcement methods due to its technical feasibility and cost effectiveness. Fiber reinforcement has a potential use in pavement layers, retaining walls, embankments, protection of slopes, stabilisation of thin soil veneers and in geotechnical earthquake engineering applications (ex: as an alternative liquefaction mitigation technique) [1-2]. Considerable amount of experimental data has been accumulated over the past few decades concerning fiber reinforced soils. Polypropylene, polyester, polyethylene, polyamide, steel and glass fibers were frequently used in these experimental studies in which effect of fiber properties (fiber type, fiber material, tensile strength, fiber length, diameter, and aspect ratio, fiber content, fiber orientation), soil properties (soil type, relative density, sand gradation, particle shape), and test parameters (normal stress in direct shear tests, effective confining pressure in triaxial tests, loading rate, effect of drained and undrained loading, effect of extension and compression loading modes, effect of isotropic compression stage, etc.) on stress-strain, volumetric and shear strength behaviour of soils were investigated. Experimental data on fiber reinforced sands was mostly obtained from drained tests. However, data is very few for undrained loading conditions which shows that fibers also perform well in granular soils for use against stability problems under undrained loading conditions like static liquefaction of slopes and embankments as well as under earthquake loading conditions by reducing the potential of excess pore pressure development, post-liquefaction settlements and lateral spreading [3-10]. So in the context of this paper, consolidated undrained triaxial testing program is conducted in order to investigate the undrained response of fiber reinforced sand in which contribution of fiber reinforcement to shear strength is evaluated

depending on strain level. It is believed this experimental data will contribute to the gap in literature especially on undrained behaviour of fiber reinforced sands.

2. EXPERIMENTAL PROGRAM

2.1 Materials

In this experimental program, river sand from Torbalı city in the boundaries of Izmir is used as the host sand material and the polypropylene fiber obtained from SİKA is used as the reinforcing fiber material. Host sand is well graded sand (SW) with relative density and grain size distribution parameters given in Table 1 and grain size distribution curve given in Figure 1. In addition, several index and strength parameters of the polypropylene fiber (Figure 2) are given in Table 2 and important ratios concerning fiber geometry and sand granulometry are also given in Table 3. Aspect ratio of the polypropylene fibers is 667 which is a high value and literature shows that high aspect ratios may provide strain-hardening stress-strain behaviour in fiber-reinforced sands.

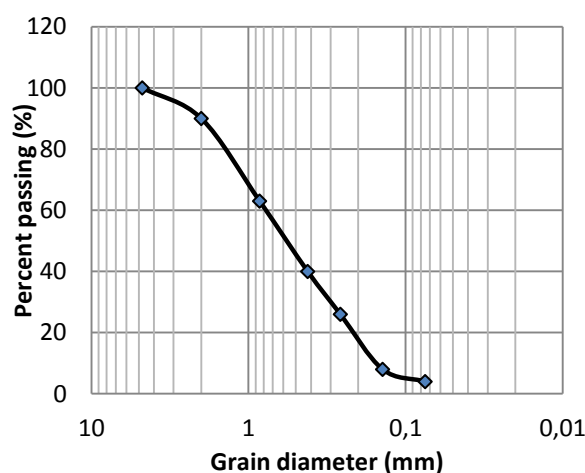


Figure 1. Grain size distribution of the host sand



Figure 2. Polypropylene fiber

Table 1. Index properties of sands used in this study.

Parameters	Soil Type SW
Relative density parameters	
Maximum dry unit weight, $\gamma_{d,max}$ (gr/cm ³)	1.79
Minimum dry unit weight, $\gamma_{d,min}$ (gr/cm ³)	1.54
Maximum void ratio, e_{max} (ASTM D4254)	0.72
Minimum void ratio, e_{min} (ASTM D4253)	0.36
Grain size distribution parameters	
Effective diameter, D_{10} , (mm)	0.13
D_{30} (mm)	0.3
D_{60} (mm)	0.8
D_{50} (mm)	0.6
Coefficient of uniformity, C_u	6.1
Coefficient of curvature, C_c	1.1

Table 2. Several index and strength parameters of polypropylene fiber.

Property	Analysis result
Color	Transparent
Diameter (micron) (Df)	18
Length (mm) (Lf)	12
Specific surface area (m ² /kg)	250
Specific gravity (gr/cm ³)	0.91
Tensile strength (N/mm ²)	300-400
Modulus of elasticity (N/mm ²)	4000

Table 3. Ratios related with fiber geometry and sand granulometry.

Ratio	Value
Aspect Ratio (Lf / Df)	667
Df / D50	0.03
Lf / D50	20

2.2 Sample Preparation and Testing Method

Consolidated undrained triaxial tests are performed on control (unreinforced) and fiber reinforced specimens at a relative density of 25% and at fiber inclusion levels of 0.5% and 1% and under three confining pressure levels 50 kPa, 100 kPa and 200 kPa. Triaxial sample dimensions were 50 mm. x100 mm. Reinforced samples were prepared at selected fiber concentrations by dry weight of sand, that is, the quantity of sand was kept unchanged when different proportions of fibers were added at a constant relative density. Fibers were mixed randomly by hand into the host sand in small increments until all the fibers were distributed uniformly within the host sand. Dry deposition method was used for compacting the sand-fiber mixture to the desired density in the split mould by slightly tamping successive layers of the mixture with a circular tamper. İbrahim et al. [9] and Freilich et al. [11] stated that the fibers tend to assume a close to horizontal orientation during mixing with dry sand and that horizontal direction is the direction of tensile strain during triaxial compression. So, it is most likely that the fibers are anisotropically distributed inside the host sand. Samples were saturated with CO₂ and back pressure methods and saturation is maintained until B values of at least 0.95 were obtained. Samples are consolidated under 50, 100 and 200 kPa effective consolidation pressures afterwhitch shearing of the specimen is conducted until obtaining constant pore

water pressure or reaching a relative axial deformation of 20%.

3. INTERPRETATION OF TEST RESULTS

3.1 Unreinforced Samples

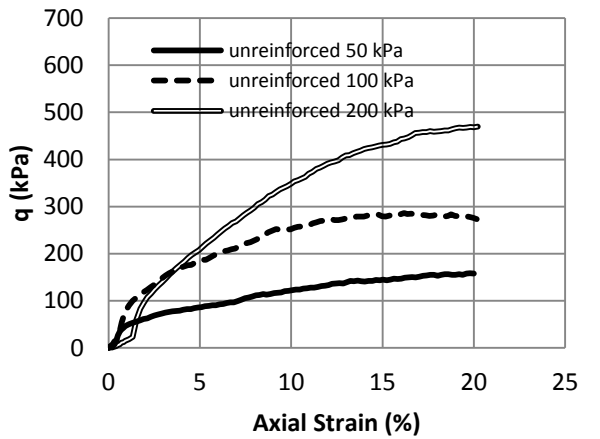
3.1.1 Deviatoric And Pore Pressure Response

Figure 3 shows the variation of deviatoric stresses, pore pressures and mobilised internal friction angles with axial strain for loose unreinforced specimens under 50, 100 and 200 kPa effective consolidation pressures. Deviator stress ($q=\sigma_1-\sigma_3=\sigma_1'-\sigma_3'$)-axial strain behaviour of all samples irrespective of consolidation pressure exhibit strain-hardening response with no noticeable peak which is typical of compacted samples (Figure 3a). Correspondingly, pore pressure responses (Figure 3b) exhibit contractive volume change tendency resulting in increase in pore pressures until axial strain level of approximately %2-%3 after which the behaviour is dominated by dilative volume change tendency decreasing the pore pressures considerably. Dilative tendency becomes more effective at lower effective confining pressures. Irrespective of consolidation pressure, unreinforced samples reached the pore pressure ratio of utmost 0.6 at axial strain levels of %2-%3.

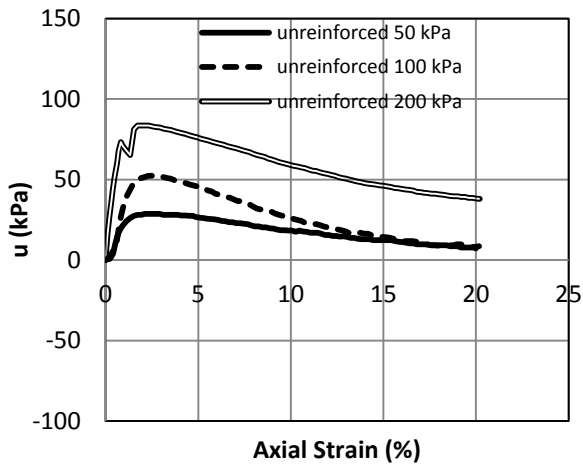
It may be expected that the host sand would exhibit more contractive tendency in loose state. Ogbonnaya et al. [12] showed that well graded sands have a great potential to exhibit contractive volume change tendency as that of poorly graded sands under undrained loading conditions. However, literature also points out that the volume change behaviour of sand is greatly influenced by the fabric formed during its deposition and sand samples prepared with the dry deposition method (the method used in this research), even the ones prepared in loose state, usually demonstrate dilative behaviour [13].

3.1.2. Undrained Effective Stress Path And Phase Transformation Line

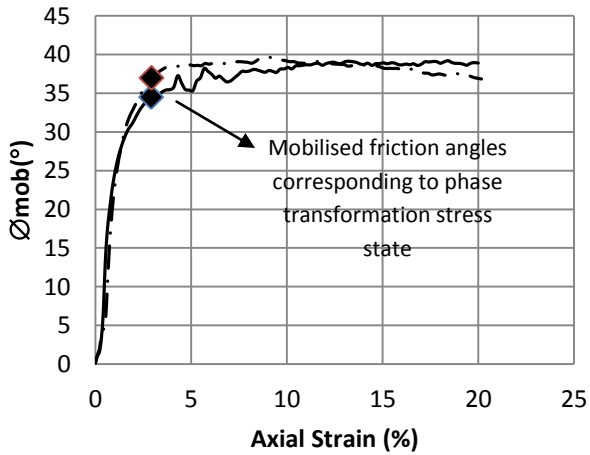
Undrained effective stress path (Figure 5) is evaluated in s' - t' stress plane representing MIT stress path convention in which $s'=(\sigma_1'+\sigma_3')/2$ represents the hydrostatic component of stress (mean effective stress) and $t'=(\sigma_1'-\sigma_3')/2$ represents the deviatoric component of stress. It is seen that loose unreinforced samples, clearly exhibit dilation tendency irrespective of consolidation pressure due to compaction during sample preparation. Phase transformation line below which stress combinations lead to volumetric contraction tendency and above which lead to volumetric dilation tendency is constructed by using the phase transformation stress states (Figure 4) [14-15]. These points are the s' - t' stress points corresponding to either the maximum pore pressure points on the pore pressure –axial strain relations or the stress states corresponding to $\delta s'=0$ on the effective stress paths for each test. Phase transformation angle has been found to be $\phi_p=36.0^\circ$ (figure 6).



(a)



(b)



(c)

Figure 3. Variation of deviator stress (a), pore pressures (b) and mobilised friction angles (c) for loose unreinforced sand

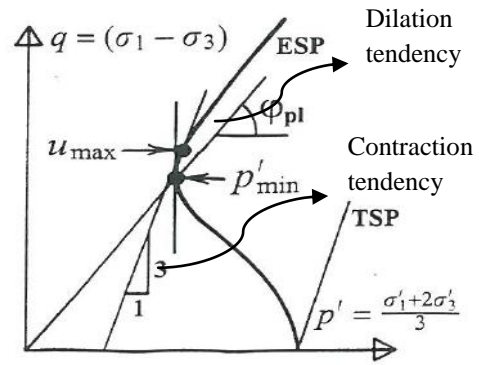


Figure 5. Schematic diagram of phase transformation state in CU triaxial test on sand [14-15]

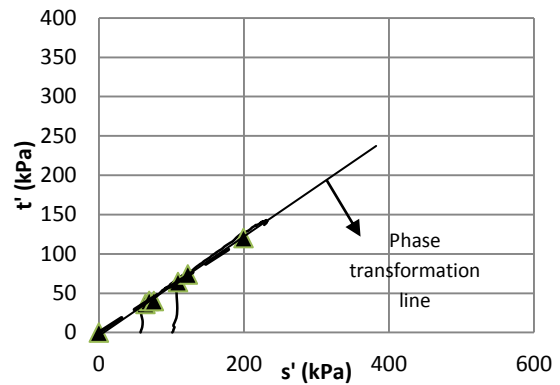


Figure 4. Undrained effective stress path for loose unreinforced samples

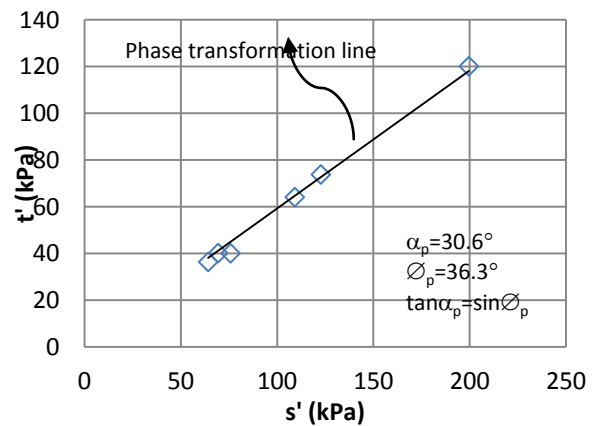


Figure 6. Phase transformation line and phase transformation angle for unreinforced samples

3.1.3 Failure Line and Shear Strength Parameters

Internal friction angles mobilised at any strain level for the loose state of the host sand is shown in Figure 3 (c). In addition, values

mobilised at phase transformation stress states (stress states at the onset of dilation tendency) is plotted with bigger and bold points in this figure. Figure 6 shows the variation of mobilised friction angles of the host sand according to effective consolidation pressure at strain level of %20. Mobilised friction angles attain higher values at 50 kPa due to dilation tendency at lower consolidation pressures. Dilation tendency is suppressed as effective consolidation pressure increase which is accompanied by a decrease in mobilised friction angles. Mohr-Coulomb shear strength parameters are determined for the limiting axial strain value of %20 since stress-strain relations exhibit strain hardening behaviour with no clear peak. Cohesion and internal friction angle of loose samples are obtained as 4.5 kPa and 36.0 (figure 8).

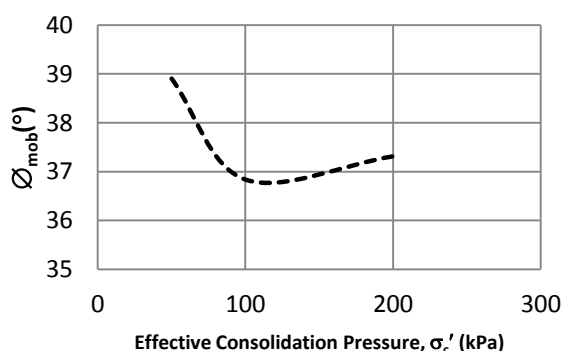


Figure 7. Variation of mobilised friction angles with effective consolidation pressure at limiting axial strain value of %20 (for the host sand)

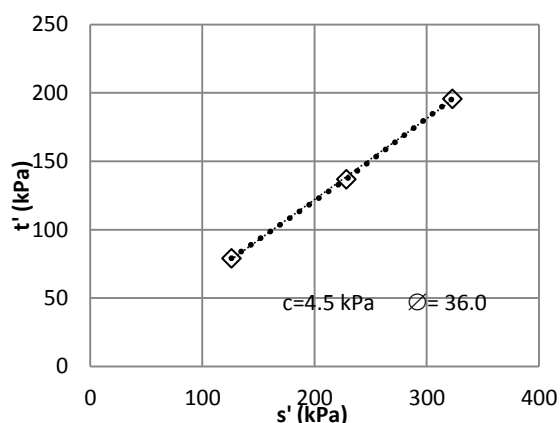


Figure 8. Effective shear strength parameters for loose and dense states of the host sand for limiting axial strain value of %20

3.2 Fiber-Reinforced Samples

3.2.1 Deviatoric And Pore Pressure Response

Typical results from consolidated undrained triaxial tests on reinforced samples under 50 kPa effective consolidation pressure is shown in Figure 9. Test results indicate that undrained stress-strain behaviours of fiber-reinforced specimens are of strain-hardening type with no clear peak irrespective of effective consolidation pressure and fiber content. Fiber reinforcement clearly enhanced the already strain-hardening behaviour of unreinforced samples. This kind of behaviour was also observed by other researchers [9,4] who stated that fiber reinforcement transforms strain-softening response into strain-hardening one preventing the occurrence of static liquefaction in saturated sands (Figure 9a)

Initial behaviour of the composite is controlled by the sand matrix, i.e. fibers begin to respond to tensile strains only after some strain level has been reached. This strain level is around %1 for 50 kPa effective consolidation pressure while under 200 kPa, it is around %5-%10 which means higher consolidation pressures may be prohibiting the activation of tensile strains and hence the stresses inside the fibers. Variation of excess pore pressure ratios with axial strain evaluates that presence of fibers cause decrease in excess pore water pressures and hence increases in effective mean stresses which are advantageous under undrained loading conditions especially for earthquake loading conditions (Figure 9 (a) and (b)). Mobilisation of friction angles with axial strain given in Figure 9 (d) demonstrate that mobilised friction angles of unreinforced samples attain higher values than reinforced ones reaching the highest values (approximately 50° at %20 axial strain) at 50 kPa effective consolidation pressure.

3.2.2 Undrained Effective Stress Paths and Phase Transformation Line

Typical undrained effective stress paths (figure 10a) for 50 kPa effective consolidation pressure show that fiber reinforced samples tend to dilate more than unreinforced ones causing pronounced increase in mean effective and deviatoric stresses of the composite material. Phase transformation stress states corresponding to onset points of dilation tendency for both reinforced and unreinforced samples irrespective of fiber content, and effective consolidation pressure are presented in Figure 11. All of the points fall on a distinct linear regression line indicating that phase transformation angle of reinforced samples is the same as that of unreinforced samples ($\phi_p=36.3^\circ$). This means the volumetric behaviour of fiber reinforced samples is governed by the same rules as that of unreinforced sand (that is a change in volumetric behaviour of the sand matrix governs). Confinement supplied by the fibers helps to increase the deviatoric stresses of the reinforced samples. In addition to that, reinforced samples exhibiting more dilative tendency than unreinforced ones is advantageous for undrained behaviour since it helps to decrease the excess pore water pressures and hence an increase is achieved in effective mean stresses giving rise to improvement of interaction between the fiber and the sand grains. Chen [4], Romero [6], and İbrahim et al. [9] as well observed the same kind of dilation tendency in their consolidated undrained triaxial tests on fiber reinforced sands.

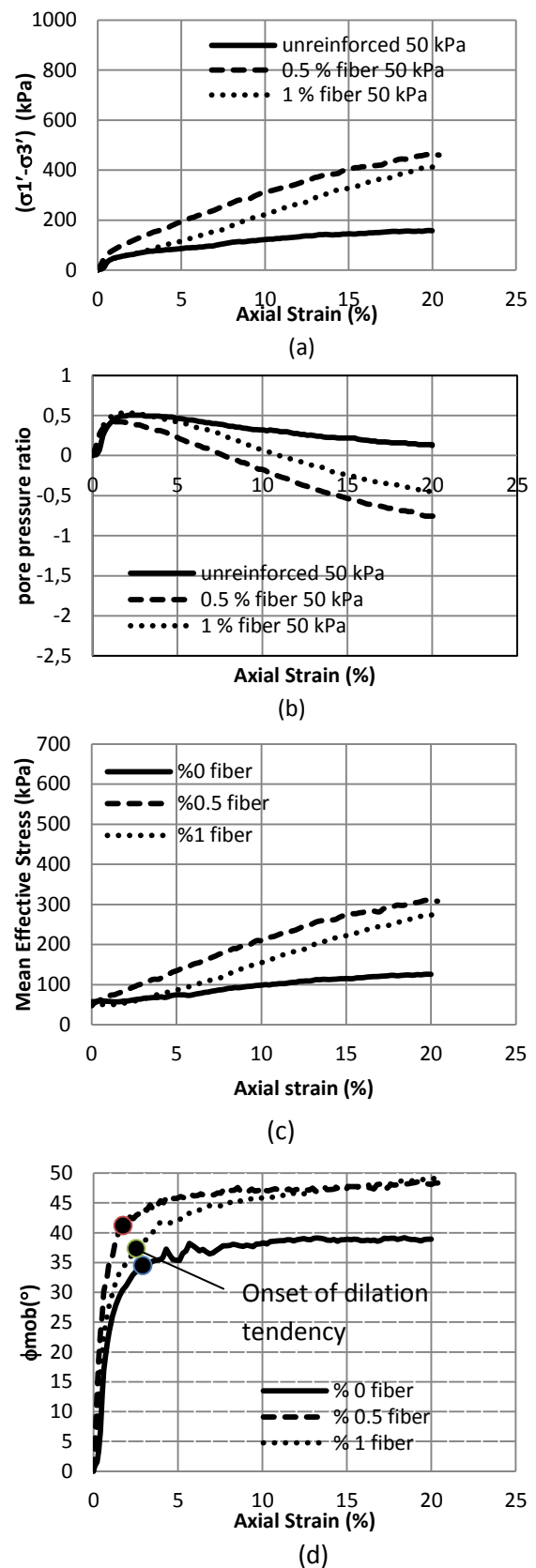
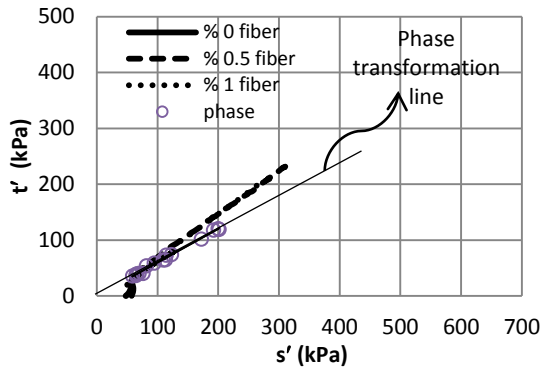
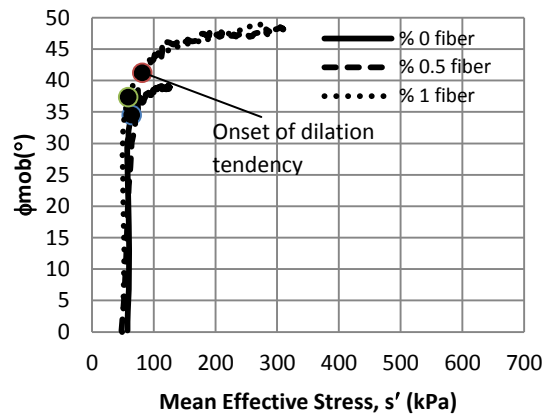


Figure 9. (a) Variation of deviator stress, (b) pore pressure ratio (c) mean effective stress and (d) mobilised friction angles at 50 kPa effective consolidation pressure



(a)



(b)

Figure 10. Undrained effective stress paths (a), mobilised friction angles (b) for 50 kPa effective consolidation pressures.

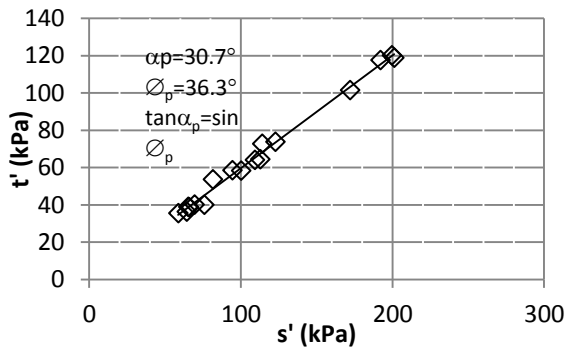


Figure 11. Phase transformation stress states and phase transformation line for both unreinforced and reinforced samples irrespective of fiber content and effective consolidation pressure

3.2.3 Shear Strength Envelopes and Shear Strength Parameters

Since fiber reinforced samples exhibit strain hardening behaviour, shear strength envelopes are evaluated at some selected axial strain levels which are. 1%, 5%, 10%, 15% and 20%. Envelopes for axial strain level of 20% in Figure 12. Apparent cohesion and internal friction angle values corresponding to the evaluated envelopes at selected strain levels are plotted in Figure 13 where it is clearly observed that mobilisation of tensile stresses and strains inside the reinforcing fibers is strongly strain-dependent. Reinforced samples exhibit linearly increasing apparent cohesion values with axial strain which are also greater than the corresponding unreinforced samples Internal friction angles are found to be lower than that for unreinforced samples, Considerable amount of decrease in friction angles values for loose state may be attributed to weaker interaction between sand grains and the fibers. Figure 14 (a) and (b) show the variation of apparent cohesion and friction angle values with fiber content. There is a linear increase in apparent cohesions and approximately linear decrease in friction angles which is reasonable.

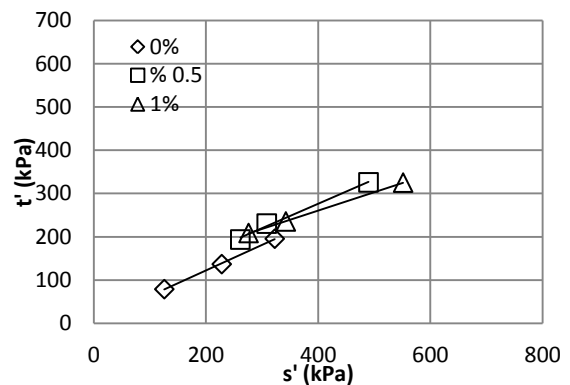


Figure 12. Shear strength envelopes at axial strain level of 20% for %0, %0.5 and %1 fiber contents

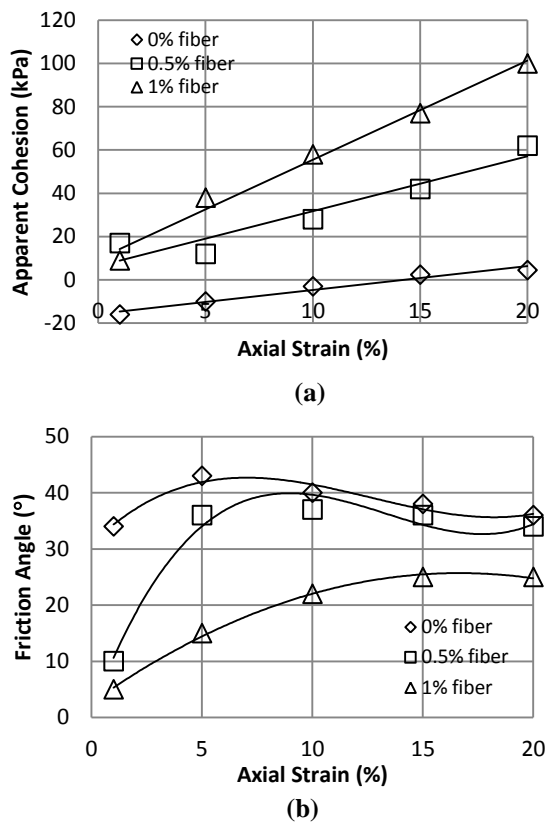


Figure 13. Apparent cohesion (a) and internal friction angle (b) values at selected axial strain levels of %1, %5, %10, %15 and %20.

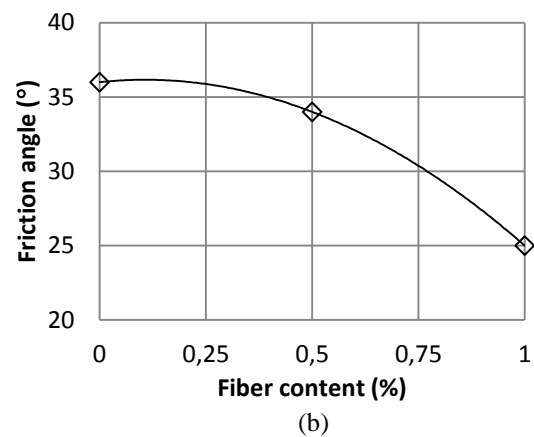
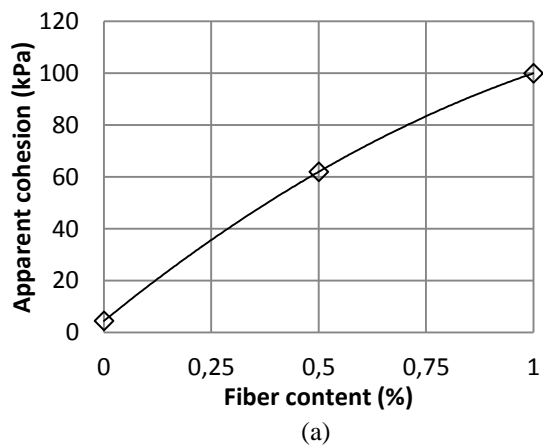


Figure 14. Variation of (a) Apparent cohesion values and (b) Internal Friction angles with fiber content at axial strain level of 20%

4. CONCLUSION

In the literature, there is considerable amount of experimental data on drained triaxial testing of fiber-reinforced sands; however, data is very few for undrained loading conditions which proved that presence of fibers absolutely improved the undrained shear strength behaviour of loose saturated sands by decreasing the excess pore water pressures and changing strain-softening stress-strain behaviour into strain-hardening one.

In the context of this paper, consolidated undrained triaxial testing program was conducted on loose sand samples reinforced with polypropylene fibers in order to contribute to the gap in undrained behaviour of fiber reinforced sands. Samples were tested under effective consolidation pressures of 50, 100 and 200 kPa and at two different fiber concentrations (0.5% and 1% by dry weight of sand). Results showed that presence of fibers caused a considerable amount of decrease in excess pore water pressures while contributing to increase in deviatoric stresses of the samples. This would only be possible if sand matrix and the fiber phase both contributed to deviatoric and hydrostatic stress state of the reinforced samples which was proved to be absolutely strain level dependent.

References

- [1] **Heyazi, S.M., Sheikhzadeh, M., Abtahi, S.M., Zadhoush, A.** (2012) “A Simple Review of Soil Reinforcement By Using Natural and Synthetic Fibers”, *Construction and Building Materials*, Vol.30, pp.100-116.
- [2] **Omarov, M.** (2010) “Liquefaction Potential and Post-Liquefaction Settlement of Saturated Clean Sands and Effect of Geofiber Reinforcement”, MSc. Thesis, University of Alaska Fairbanks, 196 p.
- [3] **Chen, C.W.** (2006). "Drained and undrained behavior of fiber-reinforced sand." Midwest Transportation Consortium of Student Papers, Transportation Scholars Conference, Iowa State University, Ames, Iowa.
- [4] **Chen, C. W.** (2007). “A constitutive model for fiber-reinforced soil.” Ph.D. thesis, Univ. of Missouri, Columbia, MO.
- [5] **Loehr, J.E., Romero, R.J., Ang, E.C.** (2005) “Development of a Strain-Based Model To Predict Strength of Geosynthetic Fiber Reinforced Soil”, *Proceedings of Geosynthetics Research and Development In Progress, Geo-Frontiers Congress 2005*, Texas, Austin, USA.
- [6] **Romero, R.J.** (2003). "Development of a constitutive model for fiber-reinforced soils." Dissertation submitted in partial fulfillment for the requirements of the Doctoral Degree, University of Missouri-Columbia.
- [7] **Diambra A, Ibraim E, Muir Wood D, Russell AR.** (2010) “Fibre Reinforced Sands: Experiments and Modelling. *Geotextiles and Geomembranes*, 28:238–250.
- [8] **Diambra A, Ibraim E, Russell AR, Muir Wood D.** (2011). “Modelling the undrained response of fibre reinforced sands”. *Soils and Foundations* 2011; 51(4):625–636.
- [9] **Ibraim E, Diambra A, Muir Wood D, Russell AR.** (2010) “Static liquefaction of fibre reinforced sand under monotonic Loading”. *Geotextiles and Geomembranes*, 28:374–385.
- [10] **Freilich B.J., Li, C., Zornberg, J.G..** (2010) “Effective Shear Strength Of Fiber Reinforced Clays”, 9th International Conference on Geosynthetics, Brazil, 2010, pp.1997-2000.
- [11] **Michalowski, RL., Cermák J.** (2003). “Triaxial compression of sand reinforced with fibers”, *ASCE Journal of Geotechnical and Geoenvironmental Engineering* 129(2), pp. 125–136.
- [12] **Ogbonnaya, I., Kyoji, S., Hiroshi, F.** (2009) “Geotechnical Properties of Sands With Varying Grading In a Stress-Controlled Ring Shear Tests, *Electronic Journal of Geotechnical Engineering*, EJGE, Vol.14.pp.1-21.
- [13] **Ishihara, K.** (1996) “Soil behaviour In Earthquake Geotechnics”, Oxford University Press, NewYork.
- [14] **İbsen, L.B., Lade, P.V.** (1998) “The Role of Characteristic Line In Static Soil Behaviour”, *Localisation and Bifurcation for soils and Rocks*, Adachi, Oda and Yashimina (eds.), Balkema, Rotterdam.
- [15] **Lade, P.V., İbsen, L.B.** (1997) “A Study of The Phase Transformation and the Characteristic Lines of Sand Behaviour”, *Symposium on Deformation and Progressive Failure In Geomechanics*, Nagoya, Japan, Soil Mechanics Paper No.12.

Recieved: 31 Dec 2014

Accepted: 7 Jan 2015